Protoplasma (2005) 225: 129–140
DOI 10.1007/s00709-005-0100-z

PROTOPLASMA
Printed in Austria

Aluminium causes variable responses in actin filament cytoskeleton of the root tip cells of *Triticum turgidum*

G. Frantzios, B. Galatis, and **P. Apostolakos***

Department of Botany, Faculty of Biology, University of Athens, Athens

Received November 25, 2004; accepted December 22, 2004; published online October 5, 2005

Summary. The effects of aluminium on the actin filament (AF) cytoskeleton of *Triticum turgidum* meristematic root tip cells were examined. In short treatments (up to 2 h) with 50–1000 μM $AlCl_3 \cdot 6H_2O$, interphase cells displayed numerous AFs arrayed in thick bundles that lined the plasmalemma and traversed the endoplasm in different directions. Measurements using digital image analysis and assessment of the overall AF fluorescence revealed that, in short treatments, the affected cells possessed 25–30% more AFs than the untreated ones. The thick AF bundles were not formed in the Al-treated cells in the presence of the myosin inhibitors 2,3-butanedione monoxime (BDM) and 1-(5-iodonaphthalene-1-sulfonyl)-1H-hexahydro-1,4-diazepine (ML-7), a fact suggesting that myosins are involved in AF bundling. In longer Al treatments, the AF bundles were disorganised, forming granular actin accumulations, a process that was completed after 4 h of treatment. In the Al-treated cells, increased amounts of callose were uniformly deposited along the whole surface of the cell walls. In contrast, callose formed local deposits in the Al-treated cells in the presence of cytochalasin B, BDM, or ML-7. These results favour the hypothesis that the actomyosin system in the Al-treated cells, among other roles, participates in the mechanism controlling callose deposition.

Keywords: Actin filament; Aluminium; Callose; *Triticum turgidum*.

Abbreviations: AF actin filament; BDM 2,3-butanedione monoxime; CB cytochalasin B; ML-7 1-(5-iodonaphthalene-1-sulfonyl)-1H-hexahydro-1,4-diazepine; MT microtubule.

Introduction

It is well known that Al severely affects plant development, mainly by inhibition of root elongation (Kochian 1995, Matsumoto 2000, Sivaguru et al. 2000a, Rout et al. 2001). Root morphogenesis is closely related to the microtubule (MT) cytoskeleton (Barlow and Parker 1996), while the onset of root cell elongation seems to be actomyosin dependent (Baluška et al. 1997). Recent research has revealed that the inhibition of root development in Al-treated plants might be related to the effects of this metal on the cytoskeleton (Matsumoto 2000, Sivaguru et al. 2000a).

Most of the available information on the effects of Al on plant cell cytoskeleton deals with MT organisation. In intact roots, Al induces (a) MT depolymerisation in the elongation zone (Sasaki et al. 1997; Sivaguru et al. 2003a, b), (b) rapid disintegration of cortical MTs in the transition zone (Horst et al. 1999, Sivaguru et al. 1999a), (c) reorganisation and stabilisation of cortical MTs in the elongation zone (Blancaflor et al. 1998), and (d) replacement of the MTs with tubulin macrotubules in root tip cells (Frantzios et al. 2000, 2001). Moreover, at different developmental stages of suspension-cultured tobacco cells, Al induces depolymerisation or stabilisation of cortical MTs (Sivaguru et al. 1999b). In the same material, short treatments with Al induce additional cortical MT bundles, while more prolonged treatments induce their depolymerisation (Schwarzerová et al. 2002).

In contrast to MTs, our knowledge of the effects of Al on the actin filament (AF) cytoskeleton is limited. In intact roots of *Zea mays*, Al induces disruption of AF arrays in the distal part of the transition zone (Sivaguru et al. 1999a) and bundling and reorientation of AF arrays in the elongation zone (Blancaflor et al. 1998). In addition, a prolonged Al treatment induces AF array disorganisation in the liverwort *Riccia fluitans* (Alfano et al. 1993) and the alga *Vaucheria longicaulis* (Alessa and Oliveira 2001), while the addition of Al to suspension-cultured soybean cells increases the tension of the AF network (Grabski and Schindler 1995).

* Correspondence and reprints: Department of Botany, Faculty of Biology, University of Athens, Athens 157 84, Greece.
E-mail: papostol@biol.uoa.gr

The present work deals with the effects of Al on the AF cytoskeleton organisation in meristematic cells of intact *Triticum turgidum* roots. This species was selected as the experimental material because it is sensitive to Al (Frantzios et al. 2000, 2001). In the *T. turgidum* root tips examined here, Al initially caused a significant increase in the number of AFs, as well as in their bundling, but later it caused their complete disruption. To investigate whether myosins are involved in the AF bundling, the effects of the myosin inhibitors 2,3-butanedione monoxime (BDM) and 1-(5-iodonaphthalene-1-sulfonyl)-1H-hexahydro-1,4-diazepine (ML-7) on the AF organisation of Al-treated cells were examined. These substances have been repeatedly used to investigate the role of myosins in plant cell processes (Komis et al. 2003, Panteris et al. 2004, Funaki et al. 2004, and references therein). Finally, considering that Al induces callose synthesis in root cells (Horst et al. 1997; Sivaguru et al. 2000a, b; Matsumoto 2000), the possible implication of the actomyosin system in the mechanism of callose deposition was investigated. Thus, the effects of the anti-AF drug cytochalasin B (CB) and of the myosin inhibitors BDM and ML-7 on the pattern of callose deposition in the Al-treated root tip cells were studied.

Material and methods

Plant material and treatments

Caryopses of *Triticum turgidum* L. var. durum Raddi were germinated on wet filter paper saturated with deionised water in petri dishes, in darkness at 25 ± 1 °C. Entire 2- to 3-day-old seedlings were treated with 50, 100, 500, and 1000 μM $AlCl_3 \cdot 6H_2O$ pre-aerated solution, pH 4.5, for 30 min, 1, 2, 4, and 8 h in darkness at 25 ± 1 °C. During treatment, the roots of the seedlings remained immersed in the Al solution. Root tips immersed in water, pH 4.5, at 25 ± 1 °C for the same time periods were used as controls. In some experiments, seedlings treated with 100 μM Al were carefully washed with distilled water and allowed to develop further for 24 to 48 h in normal conditions (darkness at 25 ± 1 °C).

To examine the sensitivity of the AF arrays to CB in the Al-treated root tips, seedlings treated with 100 μM Al for 1 h were transferred to petri dishes containing 50 μM CB in water, where they remained for 1 h. In this case, normal seedlings were used as controls, the root tips of which had been treated with 50 μM CB for 1 h.

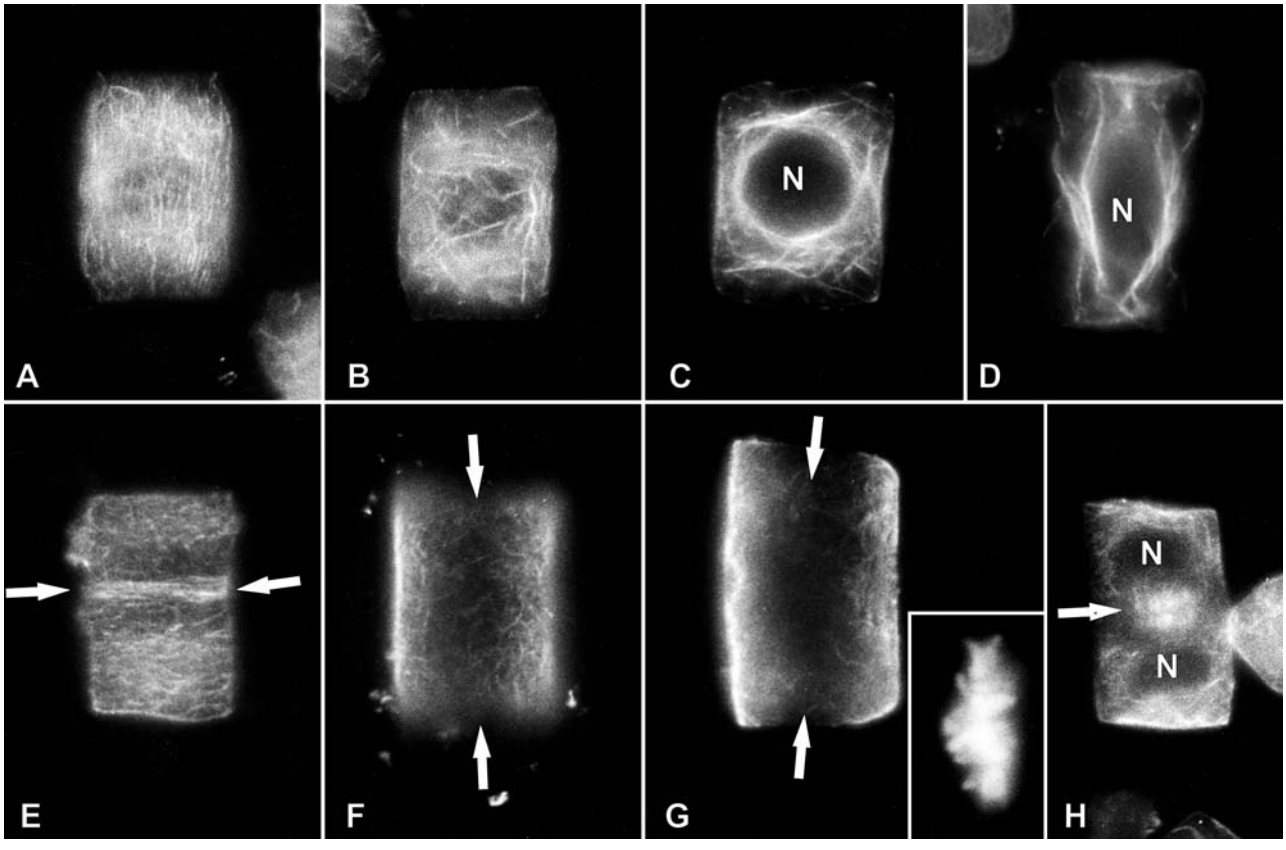

Fig. 1. Interphase (**A–D**) and dividing (**E–H**) cells of control root tips after AF staining with AlexaFluor-phalloidin. ×950. **A–D** Cortical (**A**), subcortical (**B**), and endoplasmic (**C** and **D**) interphase AF arrays. *N* Nucleus. **E** Optical section through the cortex of a preprophase cell. The arrows point to the preprophase AF band. **F** and **G** External (**F**) and median (**G**) views of a metaphase cell. The arrows indicate the areas that lack AFs. **Inset** The metaphase chromosomes as they appear after Hoechst 33258 staining. **H** Young AF phragmoplast (arrow) in a telophase cell. *N* Nucleus

To determine a possible role of myosins in the AF bundling, seedlings were initially placed in petri dishes containing 10 mM BDM in water or 5 μM ML-7 in water for 1 h. The seedlings were then transferred to petri dishes containing 100 μM Al in water enriched with 10 mM BDM or 5 μM ML-7 for 1 h.

The effects of Al on the pattern of callose deposition was studied by treatment of 2- to 3-day-old seedlings with 100 μM Al for 30 min, 1, 1.5, 2, 2.5, 3, and 5 h. Afterwards, living whole root tips were stained with 0.05% (w/v) aniline blue in 0.07 M K_2HPO_4, pH >8, to detect callose. The probable participation of the actomyosin system in callose deposition was investigated in seedlings treated as follows: (a) initial treatment with 100 μM CB for 1 h and then with 100 μM Al solution enriched with CB (100 μM); (b) initial treatment with 10 mM BDM for 1 h and then with 100 μM Al solution enriched with BDM (10 mM); or (c) initial treatment with 5 μM ML-7 for 1 h and then with 100 μM Al solution enriched with ML-7 (5 μM). In all these experiments the seedlings were treated with Al solutions for 30 min, 1, 1.5, 2, 2.5, 3, and 3.5 h.

Fluorescence microscopy

For staining of AFs, the root tips were removed and placed for 15–30 min in *m*-maleimidobezoyl-N-hydroxysuccinimide ester (100–300 μM) in microtubule-stabilising buffer (MSB) (50 mM piperazine-N,N′-bis(2-ethanesulfonic acid), 5 mM EGTA, 5 mM $MgSO_4 \cdot 7H_2O$, pH 6.8) containing 0.01–0.05% (v/v) Triton X-100. Afterwards, the root tips were fixed in 4% (w/v) paraformaldehyde in MSB for 45 min and then washed in a 1 : 1 mixture of MSB and phosphate-buffered saline (PBS). Cell walls were then digested for 50 min in 2% cellulase and 1% macerozyme in an MSB-PBS mixture (1 : 1). The enzyme mixture was enriched with AlexaFluor 568-conjugated phalloidin (Molecular Probes; 10 μl of phalloidin in 200 μl of the buffer). The root tips were then washed with MSB-PBS (1 : 1), gently squashed onto polylysine-coated coverslips and left to allow the separated cells to dry. Afterwards, the cells were incubated with MSB-PBS (1 : 1) containing AlexaFluor 568-conjugated phalloidin (10 μl of phalloidin in 200 μl of the buffer) for 90 min for AF staining. Finally, the chromatin was stained with Hoechst 33258 (Sigma; 1 μg/ml in PBS).

The specimens were examined with a Zeiss Axioplan microscope and photographed on Kodak T-MAX 400 film rated at ISO 1600.

Electron microscopy

Excised root tips from control and Al-treated seedlings were prefixed with 3% glutaraldehyde and 1% tannic acid in 0.025 M phosphate buffer (pH 7) for 2 h, postfixed with 1% OsO_4 in the same buffer overnight at 4 °C, dehydrated in an acetone series, and embedded in Spurr resin

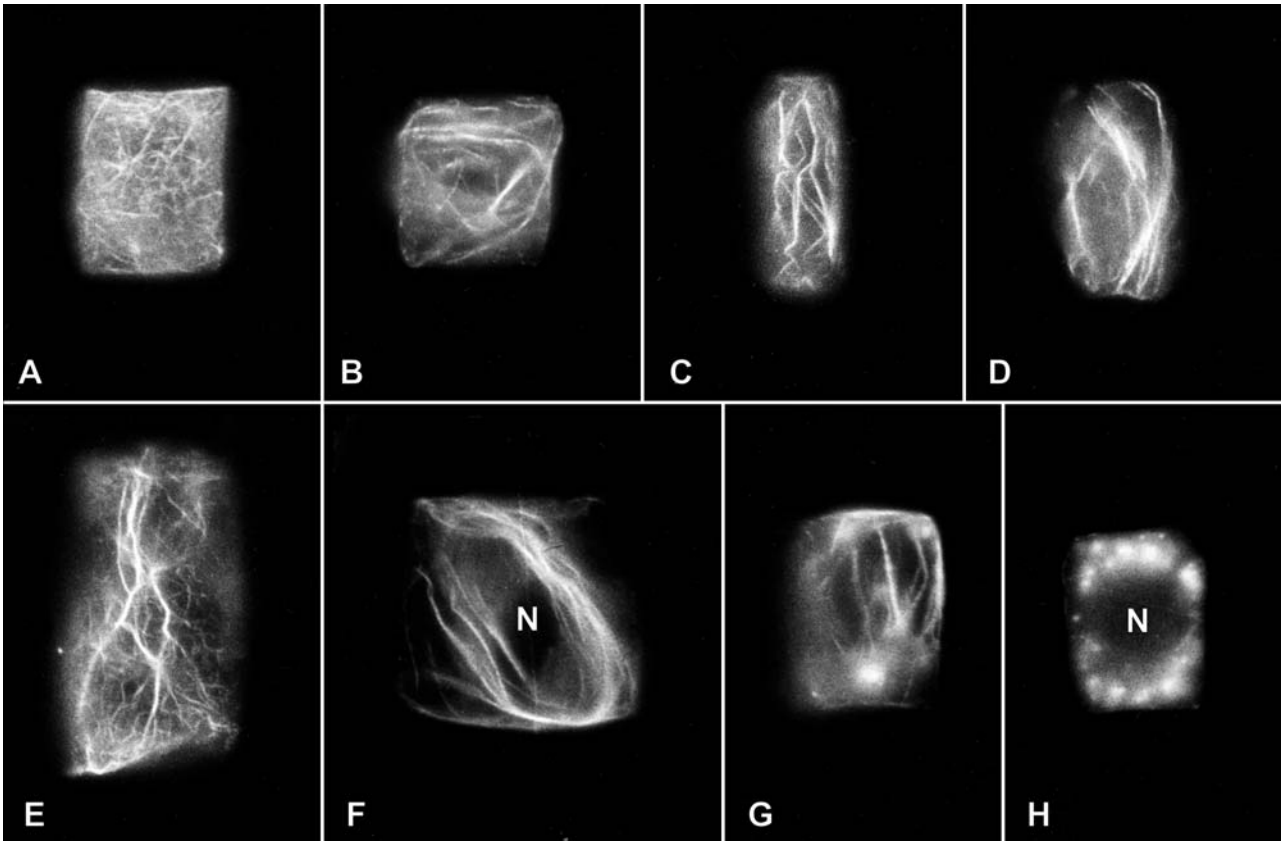

Fig. 2 A–H. Interphase Al-treated root tip cells after AF staining with AlexaFluor-phalloidin. ×950. **A–C** Cortical views of meristematic cells. Fine (**A**) and well organised (**B** and **C**) AF bundles traverse the cortical cytoplasm in different directions. Treatment: for A, 50 μM Al, 1 h; for B and C, 100 μM Al, 30 min. **D** Median view of an interphase meristematic cell. The endoplasm is traversed by thick AF bundles. Treatment: 100 μM Al, 30 min. **E** and **F** Cortical (**E**) and median (**F**) views of differentiating interphase cells. Well organised AF bundles can be observed in the cortical cytoplasm (**E**) and the endoplasm (**F**). Fine AFs can be distinguished among them. Treatment: 100 μM Al, 1 h. **G** and **H** Cortical (**G**) and median (**H**) views of interphase meristematic cells treated with 100 μM Al for 1 h (**G**) and 4 h (**H**) respectively. They display a few AF bundles and granular actin accumulations (**G**) or only granular actin accumulations (**H**). *N* Nucleus

according to the standard protocol. The thin sections were double stained with uranyl acetate and lead citrate and examined with a Philips 300 electron microscope.

Assessment of the AF content

To assess changes in the AF content due to Al treatment, image analysis either of photomicrographic negatives or directly of fluorophore-labelled specimens was applied. Although the following approaches cannot be used to quantify in absolute numbers the cellular AF content, they are reliable for a comparison of the AF content between control and Al-treated cells.

For image analysis, photomicrographic negatives of 130 control and 130 Al-treated cells were scanned through an Agfa Duoscan scanner and stored as TIFF files by Agfa FotoLook software. The Image-Pro Plus software (Media Cybernetics) was used for digital image analysis. Following background subtraction, at least five areas of predefined size were selected and the number of AFs that were automatically tracked within each were measured, averaged, and expressed as the amount of fluorescence per unit area. Background was measured in cytoplasmic areas that lacked AFs. Average fluorescence intensity per unit area of either Al-treated or control cells (arbitrary units) was plotted as a histogram by MS Excel software (Microsoft Corp.). Digital image analysis has been used previously to assess differences in the cytoskeletal element content between different cell populations (Komis et al. 2002a, b and references therein).

Differences in fluorescence intensity were also estimated by measuring the overall fluorescence of the Alexa-phalloidin-labelled cells.

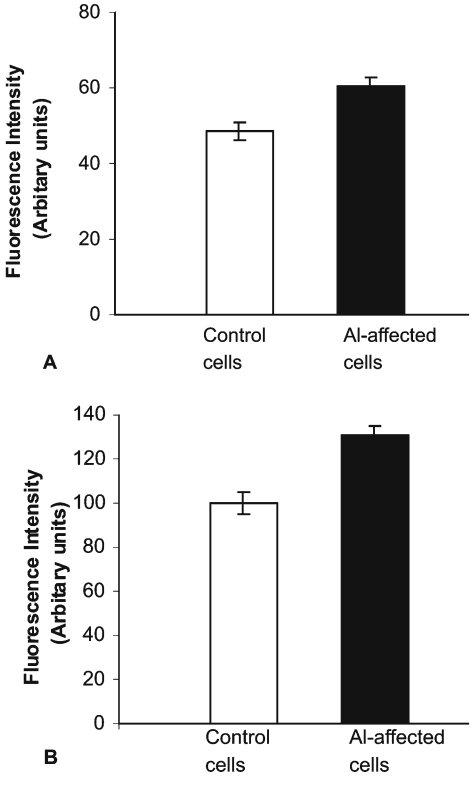

Fig. 3 A, B. Histograms showing the average AF fluorescence intensity of control interphase root tip cells (white bars) and interphase root tip cells treated with 100 μM Al for 1 h (black bars). The difference in AF fluorescence intensity between control and Al-treated cells is statistically significant ($P < 0.05$). **A** Histogram of the average AF fluorescence intensity measured through digital image analysis. Sample size: 130 control cells, 130 Al-treated cells. **B** Histogram of the average AF fluorescence intensity measured by a photometer coupled to the Zeiss Axioplan microscope, which converts fluorescence intensity to exposure time for photomicrography. Sample size: 200 control cells, 200 Al-treated cells

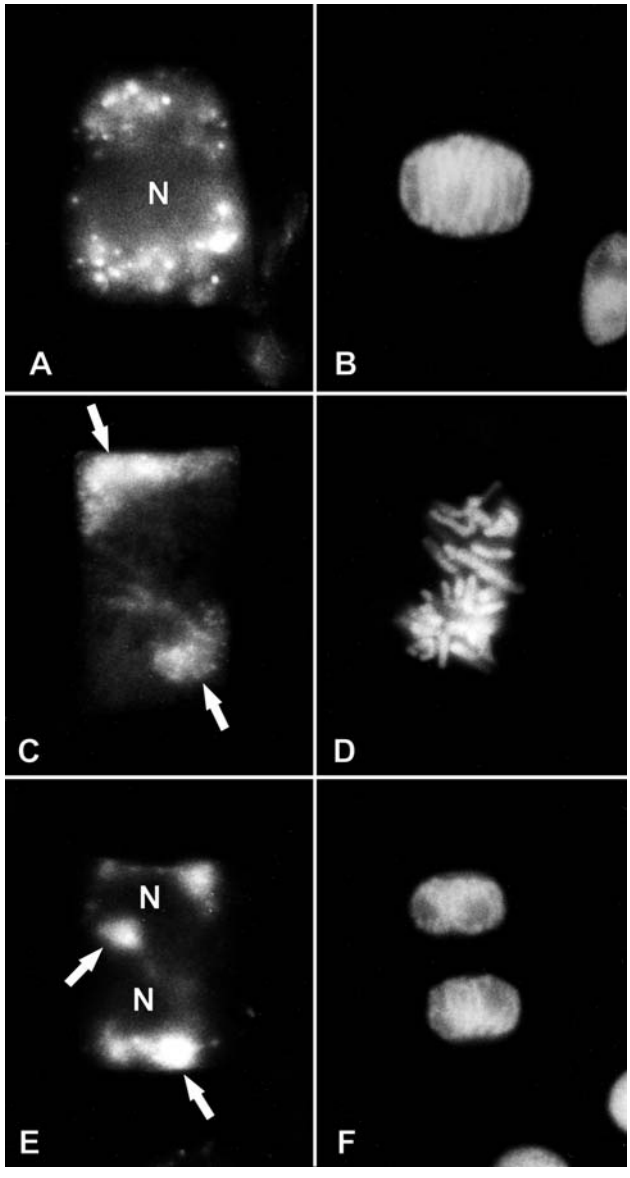

Fig. 4. Al-treated dividing root tip cells after AF staining with AlexaFluor-phalloidin (**A**, **C**, and **E**) and DNA staining with Hoechst 33258 (**B**, **D**, and **F**). *N* Nucleus. ×950. **A** and **B** Median view of an Al-treated prophase cell. **A** The cell displays granular AF accumulations localised around the nucleus, as well as in other cytoplasmic positions. **B** The prophase nucleus after Hoechst 33258 staining. Treatment: 100 μM Al, 30 min. **C** and **D** Atypical metaphase-anaphase cell showing granular actin accumulations in the polar regions (arrows in **C**). The chromosomes (**D**) are dispersed in the cell space. Treatment: 100 μM Al, 1 h. **E** Al-treated cytokinetic cell that lacks AFs but displays granular actin accumulations (arrows) in the proximity of the daughter nuclei; **F** the daughter nuclei after staining with Hoechst 33258. Treatment: 100 μM Al, 2 h

More than 200 cells from Al-treated and control seedlings were compared with a photometer coupled to the Zeiss Axioplan microscope that converts fluorescence intensity to exposure time for photomicrography. The values obtained by this approach were comparable to those obtained from digital image analysis of the photomicrographic negatives. Statistical analysis was done with the Student t-test by MS Excel software.

Results

AF organisation in control cells

The cytoplasm in interphase cells was traversed by numerous fine cortical AFs, oriented perpendicularly or parallel to the longitudinal cell axis (Fig. 1A), as well as by AFs bundles traversing the subcortical cytoplasm (Fig. 1B) and the endoplasm, mainly the perinuclear (Fig. 1C, D). In preprophase and prophase cells, a preprophase AF band was found (Fig. 1E), which persisted up to the end of prophase. During mitosis and cytokinesis, the preprophase band site remained free of AFs, forming an AF-depleted zone (Fig. 1F). In metaphase and anaphase cells, AFs were localised in all cytoplasmic cell sites, but not in the spindle interior (Fig. 1F, G). In cytokinetic cells, an AF phragmoplast was formed (Fig. 1H).

AF organisation in Al-treated cells

Interphase cells

The AF arrays were very sensitive to Al, their sensitivity depending on the Al concentration and the duration of treatment. The interphase cells treated with 50 μM Al for 30 min displayed many short, thin cortical AF bundles, randomly oriented, as well as short, thin subcortical and endoplasmic AF bundles (Fig. 2A; cf. Fig. 1A). Treatment with Al solutions at higher concentrations (100, 500, and 1000 μM) induced a stronger disturbance of the AF cytoskeleton. After 30 min of treatment, the cortical AFs formed an atypical network of very thick, randomly aligned AF bundles in most of the examined interphase cells (Fig. 2B, C, E), among which fine AFs could be distinguished (Fig. 2E). In the same cells, numerous, very thick subcortical and endoplasmic AF bundles were found aligned along the long cell axis and localised around the nucleus (Fig. 2D, F). The AF bundling that was induced by Al (Fig. 2B–F; cf. Fig. 1A–D) became more obvious after 1 h of treatment. The same phenomena were observed in cells that had undergone treatment with 50 μM Al for 1–2 h.

The Al-treated cells contained more AFs than the corresponding controls, a phenomenon detectable after short (0.5–2 h) treatments at all Al concentrations used. This AF

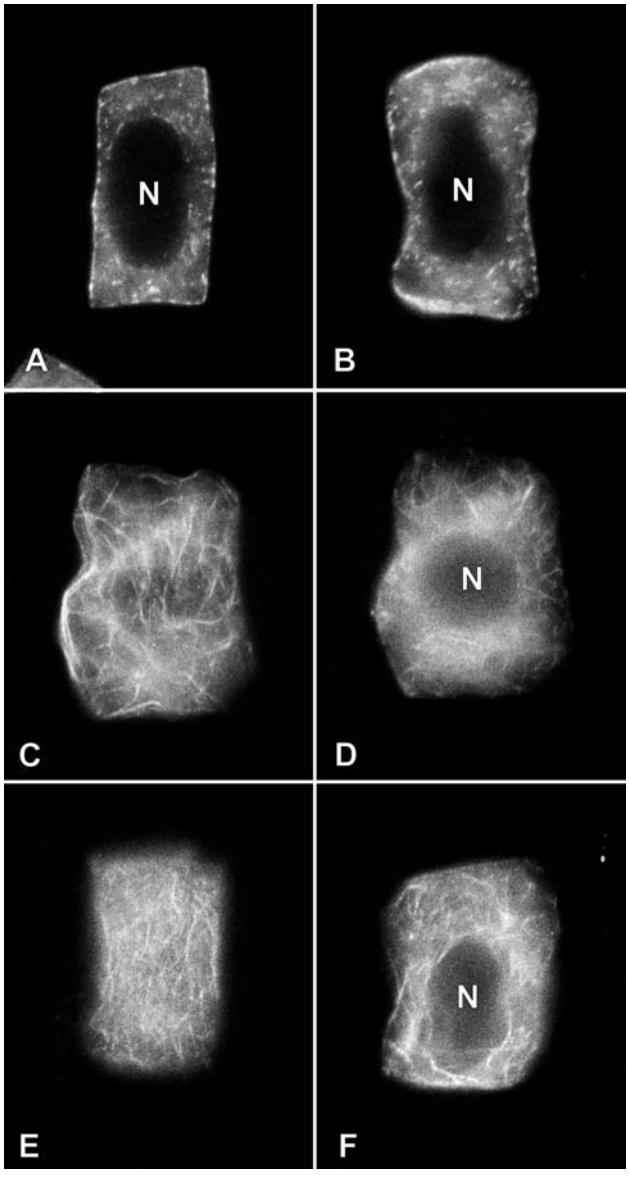

Fig. 5 A–F. Root tip cells after AF staining with AlexaFluor-phalloidin. *N* Nucleus. ×1050. **A** Control interphase cell treated with 50 μM CB for 1 h. The AFs have disintegrated (cf. Fig. 1A–D). **B** Median optical view of an interphase cell which was initially treated with 100 μM Al for 1 h and then with 50 μM CB for 1 h. It is obvious that the AF bundles which are formed in the Al-treated cells after a short treatment have disintegrated (cf. Fig. 2B–F). The cell possesses AF remnants, as in the case of control CB-treated cells (cf. Fig. 5A). **C** and **D** Cortical (**C**) and median (**D**) views of interphase cells treated with 10 mM BDM for 1 h and then with 100 μM Al plus BDM (10 mM) for 1 h. These cells lack the AF bundles that are formed in Al-treated cells (cf. Fig. 2B–F). Only fine cortical (**C**) and endoplasmic (**D**) AFs can be observed. **E** and **F** Cortical (**E**) and median (**F**) optical planes of interphase cells treated with 5 μM ML-7 for 1 h and then with 100 μM Al plus ML-7 (5 μM). The cortical cytoplasm (**E**) and the endoplasm (**F**) are devoid of the AF bundles that are formed in Al-treated cells (cf. Fig. 2B–F)

increase was quantitatively estimated by digital image analysis to be about 25%, and about 30% by the measurement of fluorescence intensity method (Fig. 3).

In more prolonged treatments, the AF bundles in the Al-treated cells became disorganised. After 4 h of treatment and at all Al concentrations used, the AF bundles disappeared and the treated cells displayed many intensely fluorescing granular actin accumulations (Fig. 2 H). These probably resulted from AF bundle disintegration. The cell shown in Fig. 2 G is in an intermediate stage of AF bundle disintegration, showing a few, poorly organised AF bundles and granular actin accumulations. AF bundle disorganisation is a gradual process that depends on the Al concentration. In root tips treated with 500 or 1000 μM Al, granular actin accumulations appeared after 30 min of treatment, while in those treated with 50 or 100 μM Al, they appeared after 1–2 h.

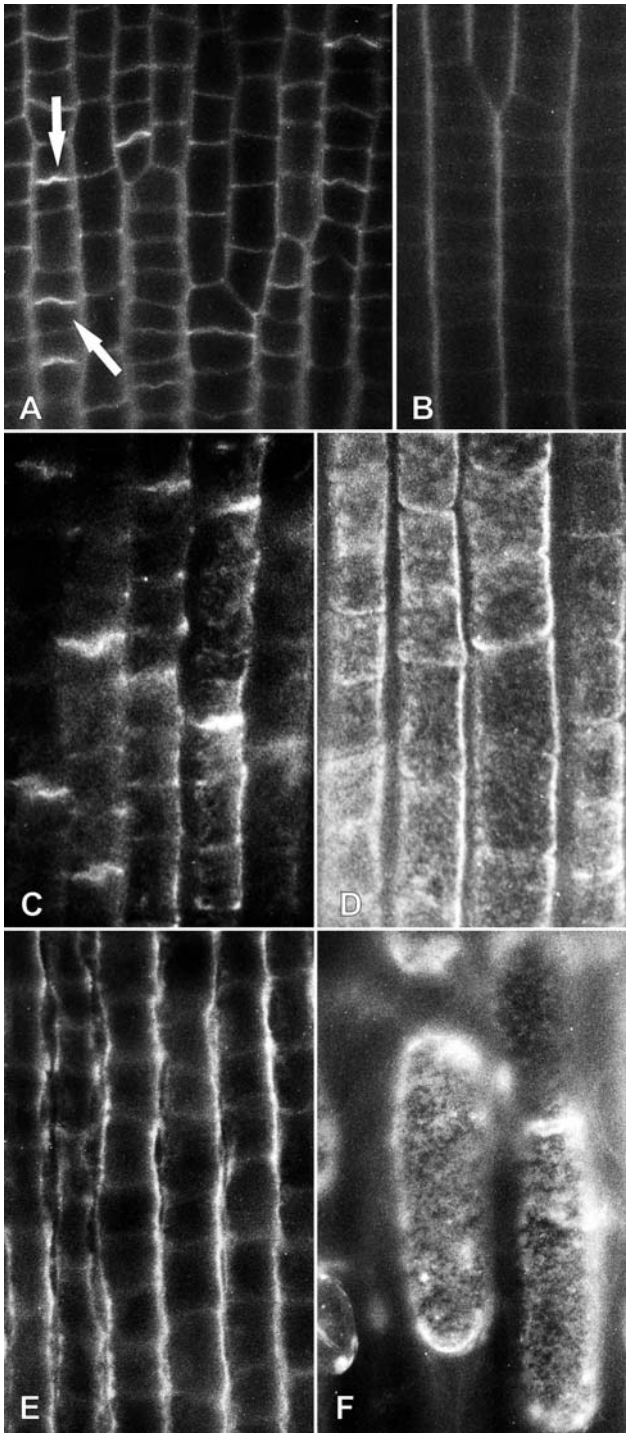

Mitotic and cytokinetic cells

The mitotic and cytokinetic cells treated with Al for 30 min to 4 h lacked AFs and displayed granular actin accumulations (Fig. 4 A, C, E; cf. Fig. 1 E–H). In preprophase and prophase cells, the actin granules were usually gathered around the nucleus, while in metaphase and anaphase cells, they were at the spindle poles (Fig. 4 A–D). In the majority of the metaphase and anaphase cells examined, the chromosome arrangement was disturbed (Fig. 4 D). This was expected because Al affects the organisation and function of the mitotic apparatus in *T. turgidum* (Frantzios et al. 2000). The Al-treated telophase and cytokinetic cells did not form an AF phragmoplast but exhibited granular actin accumulations at the polar regions, at the margins of the cell plate, and between the daughter nuclei (Fig. 4 E, F).

Recovered cells

The interphase cells which had undergone 4 h of treatment with 100 μM Al and then recovered for 24 h in normal conditions showed randomly arranged, fine AFs in the cortical cytoplasm and a perinuclear cage of AFs. After 48 h

Fig. 6. Surface views of rhizodermis from control (**A** and **B**) and Al-treated (**C–F**) root tips after aniline blue staining. **A** and **B** Rhizodermis at the meristematic (**A**) and elongation (**B**) zones of control root tips. The cell plates and the young daughter cell walls display intense callose fluorescence (arrows in **A**). The remaining cell walls do not show significant fluorescence. ×420. **C** Portion of rhizodermis at the meristematic region of an Al-treated root tip. The callose fluorescence is more intense in comparison to that of the respective region of the untreated root tips (cf. panel A). Treatment: 100 μM Al, 1 h. ×420. **D** and **E** Surface (**D**) and median (**E**) views of the rhizodermis at the elongation zone of Al-treated root tips. Numerous callose deposits can be observed uniformly distributed along the whole surfaces of the periclinal (**D**) and anticlinal (**E**) cell walls (cf. panel B). Treatment: for D, 100 μM Al, 1.5 h; for E, 100 μM Al, 2 h. D, ×500; E, ×420. **F** Optical section through the surface of two Al-treated root cap cells. Significant callose deposits are uniformly distributed along the whole surface of the cell walls. Treatment: 100 μM Al, 1 h. ×420

of recovery, the interphase and dividing Al-treated cells exhibited the typical AF organisation (data not shown).

Treatment of Al-treated root tips with CB and myosin inhibitors

CB treatment

Control root tip cells treated with CB for 1 h showed no AFs, only AF remnants in different cell sites (Fig. 5A). The AF bundles in the Al-treated cells exhibited the same sensitivity to CB. After 1 h of CB treatment, these cells possessed AF remnants only (Fig. 5B). Therefore, in contrast to Al-treated *Zea mays* roots (Blancaflor et al. 1998), the AF bundle arrays in Al-treated *T. turgidum* cells do not show an increased resistance to CB.

Treatment with myosin inhibitors

Root tip cells treated with 10 mM BDM for 1 h and then with 100 μM Al supplemented with BDM (10 mM) for 1 h were characterised by the presence of numerous, thin cortical and endoplasmic AFs (Fig. 5C, D). However, these AFs did not form thick bundles, like those found in the root tip cells treated with Al alone (Fig. 5C, D; cf. Fig. 2A–F). Moreover, the root tip cells treated with 5 μM ML-7 for 1 h and then with 100 μM Al supplemented with ML-7 (5 μM) for 1 h were devoid of AF bundles but possessed a rich network of fine cortical and endoplasmic AFs (Fig. 5E, F; cf. Fig. 2A–F). Therefore, the myosin inhibitors inhibit the AF bundling induced by Al.

Patterns of callose deposition in root tip cells

Control and Al-treated root tips

The control whole root tips showed intense callose fluorescence after aniline blue staining in the cell plates and the young rhizodermal cell walls (Fig. 6A). In contrast, the mature rhizodermal cell walls in the meristematic region and in the elongation zone exhibited low aniline blue fluorescence (Fig. 6B).

Treatment with 100 μM Al for 30 min to 5 h caused a significant increase in the aniline blue fluorescence in all the rhizodermal cell walls (Fig. 6C–F; cf. Fig. 6A, B), a phenomenon indicating the induction of callose deposition. The intensity of the fluorescence in the cell plates and the young daughter cell walls was greater than that in the untreated root tips (Fig. 6C; cf. Fig. 6A). In addition, granular callose deposits were localised along the whole surface of the periclinal walls of the rhizodermal cells in the meristematic and elongation zones (Fig. 6D, F). Intense callose deposition also occurred along the whole surface of the anticlinal walls of the rhizodermal cells (Fig. 6E; cf. Fig. 6B). Transmission electron microscopy examination revealed that the walls of the internal cell layers displayed local deposits containing electron-transparent material (Fig. 7A; cf. Fig. 7C), which probably represents callose.

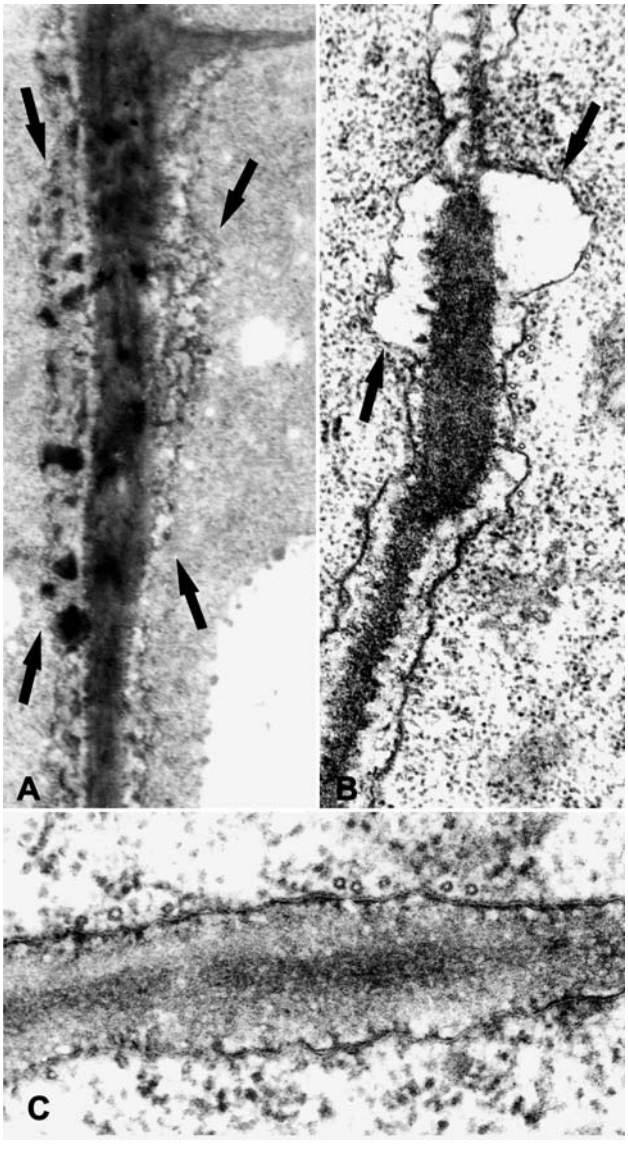

Fig. 7. Electron micrographs of walls of inner cells from Al-treated (**A** and **B**) and control (**C**) root tips as they appear in longitudinal sections. **A** The arrows point to local cell wall deposits consisting of materials displaying varying electron densities. Treatment: 1000 μM Al, 8 h. ×14000. **B** The arrows mark regions of plasmalemma detached from the cell wall. Treatment: 1000 μM Al, 8 h. ×35000. **C** Cell wall region from a control root tip cell. ×65000

Al-treated root tips treated with CB and myosin inhibitors

In the Al-treated root tips in which the AFs were disintegrated after CB treatment, intense callose deposition was found in the cell plates and the young daughter cell walls (Fig. 8A). In the same root tips, callose was deposited on the walls of all rhizodermal cell types in the meristematic and elongation zones (Fig. 8A, B). However, in contrast to the root tips treated with Al alone, these callose deposits were not uniformly distributed along the walls (Fig. 8A, B; cf. Fig. 6C–F).

In addition, inhibition of myosin activity disturbed the pattern of callose deposition in the Al-treated root tips (Fig. 8C–F; cf. Fig. 6D–F). In the presence of BDM or ML-7, the rhizodermal cells of the Al-treated root tips formed numerous local callose deposits (Fig. 8C–F). Therefore, the AF disorganisation and the inhibition of myosin activity disturb the pattern of callose deposition in Al-treated root tips.

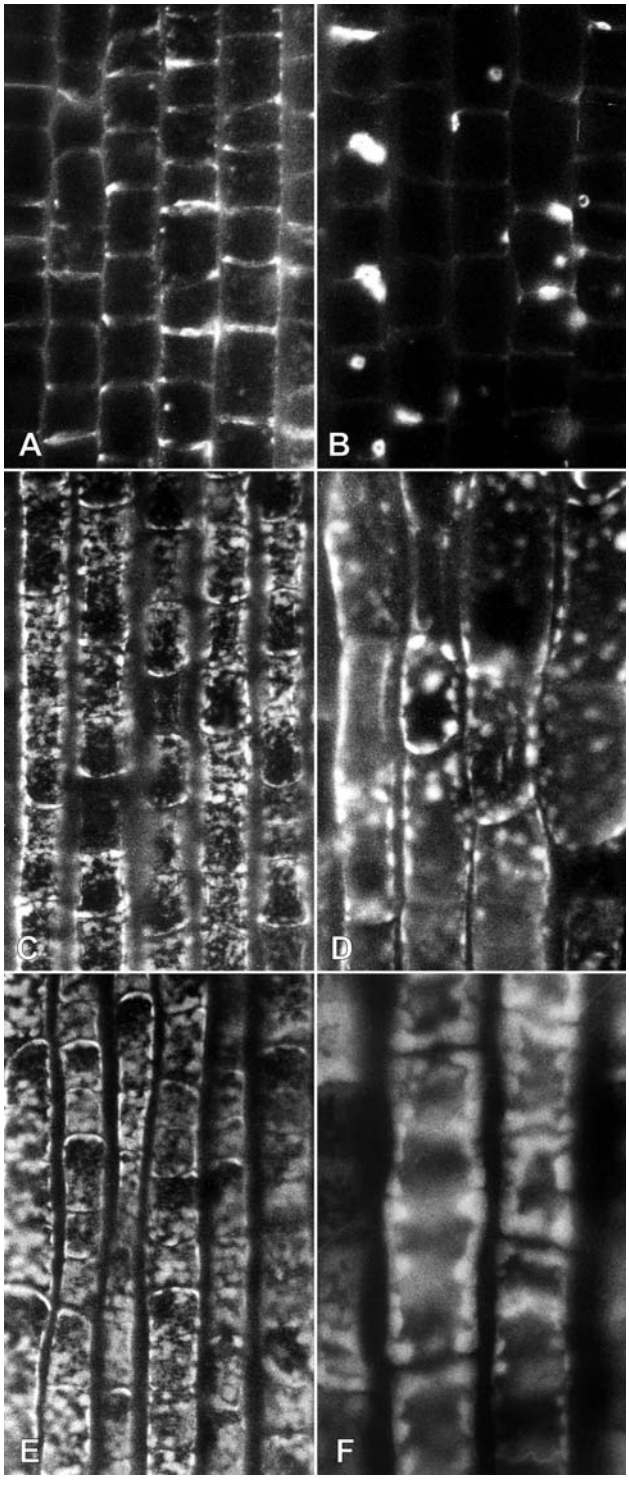

Discussion

Increase in AF number

One of the main findings of this work is that short Al treatments (0.5–2 h) induce a significant increase in the number of AFs in interphase root tip cells (Fig. 3). This increase could be attributable either to the direct interference of Al with the polymerisation process of granular actin or to its effect on the mechanisms controlling AF dynamics. In the latter case, the AFs may gain a longer lifetime compared to that of AFs in control cells. According to Grabski et al. (1998), Al toxicity could be related to the ability of Al to maintain the AF network in an assembled state, while according to Sivaguru et al. (1999a), the overall increase in the intensity of actin fluorescence in Al-treated *Zea mays* root cells indicates that AF polymerisation is altered upon exposure to Al.

It is known that Al^{3+} replaces Mg^{2+} and forms the complexes Al^{3+}-ATP and Al^{3+}-GTP, which are hydrolysed 10^5 times more slowly than Mg^{2+}-ATP and Mg^{2+}-GTP (MacDonald et al. 1987). The dynamic condition of AFs depends on the ability of granular actin to bind to a nucleotide

Fig. 8. Surface views of rhizodermal areas taken from the examination of Al-treated whole root tips, additionally treated with an anti-AF drug (**A** and **B**) or two myosin inhibitors (**C–F**). The root tips were stained with aniline blue. **A** and **B** View of rhizodermal cells from the elongation zone of root tips treated with 100 μM CB for 1 h and then with 100 μM Al plus CB (100 μM) for 2 h. The cells exhibit intense, local callose deposits which are randomly distributed (cf. Fig. 6D–F). ×420. **C–F** Rhizodermal cells of the elongation zone of Al-treated root tips, further treated with BDM (**C** and **D**) and ML-7 (**E** and **F**). Numerous, local, randomly distributed callose deposits can be observed (cf. Fig. 6D–F). Treatment: for C and D, 10 mM BDM, 1 h, and then 100 μM Al plus 10 mM BDM, 2 h; for E and F, 5 μM ML-7, 1 h, and then 100 μM Al plus 5 μM ML-7, 2 h. C and E, ×420; D and F, ×1050

(i.e., ATP or ADP) and to Mg^{2+} or Ca^{2+}, as well as to hydrolyse the complexes Mg^{2+}-ATP and Mg^{2+}-GTP (Vantard and Blanchoin 2002). The replacement of Mg^{2+} with Al^{3+} might affect AF dynamics (Grabski and Schindler 1995), favouring their longevity and thereby probably leading to the increase in AF number in the Al-treated cells.

Alternatively, the increased number of AF in the Al-treated cells may be attributable to a disturbance of actin-binding proteins that control AF dynamics. The activity of these proteins is controlled by pH, cytosolic Ca^{2+}, the Ca^{2+}/calmodulin complex and different signal transduction processes (Gibbon 2001, Vantard and Blanchoin 2002). The Al interference with AF dynamics can be explained using the above information and the fact that Al disturbs the homeostasis of cytosolic Ca^{2+} (Rengel and Zhang 2003), changes the cytosolic pH (Lindberg and Strid 1997), and inhibits phospholipase activity (Jones and Kochian 1995).

In our opinion, the disturbance of Ca^{2+} homeostasis induced by Al is probably the main factor triggering the increase in the AF number in the affected cells. Higher cytosolic Ca^{2+} concentrations promote granular actin polymerisation (Strzelecka-Golaszewska 2001). Moreover, the effects of Al on the cytosolic pH (Lindberg and Strid 1997) might induce AF elongation. AF elongation in tip-growing cells is predicted to be maximal in cytoplasmic regions with alkaline pH (Gibbon 2001).

AF bundling

Short Al treatments not only induced an increase in the number of AFs in interphase cells but also AF bundling. AF bundling following Al treatment has been described in *Zea mays* root tip cells (Blancaflor et al. 1998, Sivaguru et al. 1999a) and in the alga *Vaucheria longicaulis* (Alessa and Oliveira 2001). In addition, Grabski and Schindler (1995) and Grabski et al. (1998) suggested that the increase in AF rigidity in Al-treated cultured soybean cells is related to AF bundling (see also Arnoys and Schindler 2000). AF bundling is a common response of animal cells to mechanical stress (Galbraith et al. 1998) and of plant cells to hyperosmotic conditions (Komis et al. 2002a, 2003).

The AF bundling in Al-treated cells may be induced by myosins and by other Ca^{2+}-dependent, actin-related proteins (Grabski et al. 1998, Alessa and Oliveira 2001). The Al-induced disturbance of Ca^{2+} homeostasis (Rengel and Zhang 2003) probably affects the activity of these proteins, resulting in the formation of AF bundles (Sivaguru et al. 1999a, Alessa and Oliveira 2001). In addition, Al induces transcription of fimbrin genes in *Triticum aestivum* (Cruz-Ortega et al. 1997). Fimbrin induces AF bundling. Plant cells responding to Al stress probably form fimbrin that bundles the AFs to secure their integrity.

Our data show that myosins are also involved in AF bundling. The inhibition of myosin activity by BDM, a general inhibitor of myosin ATPase (Hermann et al. 1992), and ML-7, a specific inhibitor of myosin light-chain kinase (Satoh et al. 1987), prevents the assembly of the thick AF bundles in Al-treated cells (Fig. 5C–F). Myosin involvement in AF bundling is well documented in animal cells (Verkhovsky et al. 1995, Krendel and Bonder 1999) and has been shown in plant cells under hyperosmotic stress (Komis et al. 2003).

It should be noted here that, according to Ostap (2002), BDM is not a general myosin inhibitor because it inhibits the skeletal muscle myosin II, but not the ATPase activity of animal myosins I, V, and VI. However, the fact that BDM inhibits the activity of myosin V in vivo and in vitro (Uemura et al. 2004), as well as that of the plant myosin XI (Tominaga et al. 2000, Funaki et al. 2004), suggests that it can be considered as a general inhibitor of myosins. Regarding ML-7, the arguments for its use in investigating the role of myosins in plant systems have been recently discussed (Panteris et al. 2004).

AF disorganisation

Another finding of this study is that the increases in AF number and the bundling in Al-treated cells are followed by AF disorganisation. The most sensitive AFs are those of mitotic and cytokinetic cells, in which AF disorganisation is completed within the first hour of treatment. In interphase cells, AF disorganisation starts after 30 min of treatment and is completed after 4 h. The temporary AF resistance to the toxic action of Al in interphase cells can be attributed to AF bundling (see Arnoys and Schindler 2000).

AF disorganisation in the Al-treated plant cells probably represents a more general phenomenon. It has been described in *Zea mays* root cells (Sivaguru et al. 1999a), in the liverwort *Riccia fruitans* (Alfano et al. 1993), and in the alga *Vaucheria longicaulis* (Alessa and Oliveira 2001). In these plants, AF disorganisation commences after 30 min of Al treatment and is completed after 8–16 h. This disintegration probably occurs because Al affects the dynamic condition of AFs by disturbing the cytosolic Ca^{2+} concentration (Sivaguru et al. 1999a, Alessa and Oliveira 2001), interfering with the inositol 1,4,5-triphosphate signal transduction pathway (Sivaguru et al. 1999a), and causing disorder of the cell wall–plasmalemma integrity (Horst et al. 1999; Sivaguru et al. 1999a, 2000a). Although all these mechanisms might function in the

Al-treated *T. turgidum* root cells, the most probable candidate for AF disorganisation is the change in the cytosolic Ca^{2+} concentration. The activities of many proteins that regulate AF dynamics are controlled by cytosolic Ca^{2+} (Gibbon 2001, Vantard and Blanchoin 2002).

AF behaviour in the Al-treated *T. turgidum* root tip cells raises the following questions. (a) Why does the sensitivity of AFs to Al differ between interphase and dividing cells? (b) Why does Al initially induce an increase in AF number in short treatments, while later it induces AF disorganisation? Regarding the first question, it seems likely that, similar to MTs (Hepler and Hush 1996), the AFs in mitotic and cytokinetic cells are more dynamic than those of interphase cells and are thus more sensitive to Al. Regarding the second question, it is probable that Al creates intracellular, AF-affecting conditions that change during treatment. For instance, the cytosolic Ca^{2+} concentration increases continuously during Al treatment (Rengel and Zhang 2003 and references therein). At the beginning of the treatment, the cytosolic Ca^{2+} concentrations promote AF formation and bundling, but those prevailing later induce AF disorganisation. It is known that very high Ca^{2+} concentrations induce AF disorganisation (Janmey 1994). Similarly, 1 h of Al treatment of cultured tobacco cells induces an increase in the number of cortical MT bundles of about 20–25%. This phenomenon has been correlated to increased levels of α-tubulin (in its tyrosinated form) and elements of the tubulin-folding chaperone CCT. However, 6 h of Al exposure results in extensive disorganisation of cortical MT bundles and decreased levels of α-tubulin, tyrosinated tubulin, and CCTs (Schwarzerová et al. 2002).

Callose deposition

In this work, it was found for the first time that AF disorganisation and the inhibition of myosin activity disturb the pattern of callose deposition in Al-treated *T. turgidum* root tip cells (Fig. 8A–F; cf. Fig. 6C–F). Callose is synthesized on the external plasmalemma surface by the 1,3-glucan synthase, which is localised within the membrane (McCormack et al. 1997). The cytosolic Ca^{2+} regulates the glucan synthase activity (Kudlicka and Brown 1997). The change in the pattern of callose deposition in Al-treated cells additionally treated with CB, BDM, and ML-7 may mirror the change in the callose synthase distribution in the plasmalemma. In cells treated only with Al, the actomyosin system mediates a more or less symmetrical distribution of callose synthases in the plasmalemma. AF participation in the distribution of the biomembrane proteins is well established in animal (Baumann 2001) and plant cells (Shaw and Quatrano 1996). In particular, according to Volkmann and Baluška (1999), the plant AF cytoskeleton communicates with the cell periphery, especially when the plasmalemma-associated synthase complexes support callose formation.

Role of the atypical AF arrays

The atypical AF arrays may also be implicated in the mechanisms by which the plant reduces the toxic action of Al. The plants reduce this toxicity by secreting organic anions which bind to Al^{3+}, mainly malic ions, into the rhizosphere (Matsumoto 2000, Ma et al. 2001, Ryan et al. 2001), by activating plasmalemma channels transporting anions (Delhaize and Ryan 1995, Ma et al. 2001, Ryan et al. 2001, Zhang et al. 2001).

The cytoskeleton in animals and plants, among other functions, controls the function of the ion channels in the plasmalemma. In the former, the cortical AFs control the activity of K^+ and Na^+ channels (Papakonstanti et al. 2000, Szaszi et al. 2000), while in the latter, these cytoskeletal elements are involved in the stomatal movement regulating the activity of the K^+ channels in the plasmalemma of guard cells (for references, see Galatis and Apostolakos [2004]). Therefore, the well-organised AF arrays formed at the beginning of Al treatment possibly participate in the activation of ion channels in the plasmalemma that reduce Al toxicity. After AF disintegration, the tubulin macrotubules that replace MTs in the affected cells and resist Al (Frantzios et al. 2000, 2001) could take on this activity.

The cortical AF arrays in the Al-treated cells may also protect the plasmalemma, which, according to Matsumoto (2000), is strongly stressed by Al. This stress is structurally expressed by plasmalemma detachment from the cell wall (Clune and Copeland 1999, Minocha et al. 2001), a phenomenon also observed in *T. turgidum* (Fig. 7B; cf. Fig. 7C). In animal cells under mechanical stress, the cytoskeleton protects the structural and functional integrity of the plasma membrane, forming well-organised MT and AF cortical arrays (Ingber 1997, Katoh et al. 1998, Ko and McCulloch 2000). The plant cytoskeleton seems to behave similarly (Komis et al. 2002a, b, 2003). The change in the pattern of callose deposition in Al-treated cells in the absence of AFs suggests that the AFs are involved in the functional integrity of the plasmalemma.

Acknowledgments

The financial support to G. Frantzios by the Bodosakis Foundation is gratefully acknowledged. We thank M. Issidorides for allowing access to the digital image analysis facilities of the Cozzica Foundation, Greece,

M. Zachariadis for his assistance in preparation of the plates, and C. Katsaros for critical reading of the manuscript. This study was partially supported by grants from the University of Athens, the Hellenic Ministry of National Education and Religious Affairs, and the EU, within the framework of the Operational Programme for Education and Initial Vocational Training (O.P. "Education'', project "Pythagoras'').

References

Alessa L, Oliveira L (2001) Aluminum toxicity studies in *Vaucheria longicaulis* var. macounii (Xanthophyta, Tribophyceae). II. Effects on the F-actin array. Environ Exp Bot 45: 223–237

Alfano F, Russell A, Gambardella R (1993) The actin cytoskeleton of the liverwort *Riccia fluitans*: effects of cytochalasin B and aluminium ions on rhizoid tip growth. J Plant Physiol 142: 569–574

Arnoys EJ, Schindler M (2000) Aluminum modifies the viscosity of filamentous actin solutions as measured by optical displacement microviscometry. Anal Biochem 277: 1–10

Baluška F, Vitha S, Barlow PW, Volkmann D (1997) Rearrangements of F-actin arrays in growing cells of intact maize root apex tissues: a major developmental switch occurs in the postmitotic transition region. Eur J Cell Biol 72: 113–121

Barlow PW, Parker JS (1996) Microtubular cytoskeleton and root morphogenesis. Plant Soil 187: 23–36

Baumann O (2001) Disruption of actin filaments causes redistribution of ryanodine receptor Ca^{2+} channels in honeybee photoreceptor cells. Neurosci Lett 306: 181–184

Blancaflor EB, Jones DL, Gilroy S (1998) Alterations in the cytoskeleton accompany aluminum-induced growth inhibition and morphological changes in primary roots of maize. Plant Physiol 118: 159–172

Clune TS, Copeland L (1999) Effects of aluminium on canola roots. Plant Soil 216: 27–33

Cruz-Ortega R, Cushman JC, Ownby JD (1997) cDNA clones encoding 1,3-β-glucanase and a fimbrin-like cytoskeletal protein are induced by Al toxicity in wheat roots. Plant Physiol 114: 1453–1460

Delhaize E, Ryan PR (1995) Aluminum toxicity and tolerance in plants. Plant Physiol 107: 315–321

Frantzios G, Galatis B, Apostolakos P (2000) Aluminium effects on microtubule organization in dividing root-tip cells of *Triticum turgidum*. I. Mitotic cells. New Phytol 145: 211–224

– – – (2001) Aluminium effects on microtubule organization in dividing root-tip cells of *Triticum turgidum*. II. Cytokinetic cells. J Plant Res 114: 157–170

Funaki K, Nagata A, Akimoto Y, Shimada K, Ito K, Yamamoto K (2004) The motility of *Chara corallina* myosin was inhibited reversibly by 2,3-butanedione monoxime (BDM). Plant Cell Physiol 45: 1342–1345

Galatis B, Apostolakos P (2004) The role of the cytoskeleton in the morphogenesis and function of stomatal complexes. New Phytol 161: 613–639

Galbraith CG, Skalak R, Chien S (1998) Shear stress induces spatial reorganization of the endothelial cell cytoskeleton. Cell Motil Cytoskeleton 40: 317–330

Gibbon BC (2001) Actin monomer-binding proteins and the regulation of actin dynamics in plants. J Plant Growth Regul 20: 103–112

Grabski S, Schindler M (1995) Aluminum induces rigor within the actin network of soybean cells. Plant Physiol 108: 897–901

– Arnoys E, Busch B, Schindler M (1998) Regulation of actin tension in plant cells by kinases and phosphatases. Plant Physiol 116: 279–290

Hepler PK, Hush JM (1996) Behavior of microtubules in living plant cells. Plant Physiol 112: 455–461

Herrmann C, Wray J, Travers F, Barman T (1992) Effect of 2,3-butanedione monoxime on myosin and myofibrillar ATPases: an example of an uncompetitive inhibitor. Biochemistry 31: 12227–12232

Horst WJ, Püschel A-K, Schmohl N (1997) Induction of callose is a sensitive marker for genotypic aluminium sensitivity in maize. Plant Soil 192: 23–30

– Schmohl N, Baluška F, Sivaguru M (1999) Does aluminium affect root growth of maize through interaction with the cell wall-plasma membrane-cytoskeleton continuum? Plant Soil 215: 163–174

Ingber DE (1997) Tensegrity: the architectural basis of cellular mechanotransduction. Annu Rev Physiol 59: 575–599

Janmey PA (1994) Phosphoinositides and calcium as regulators of cellular actin assembly and disassembly. Annu Rev Physiol 56: 169–191

Jones DL, Kochian LV (1995) Aluminum inhibition of the inositol 1,4,5-trisphosphate signal transduction pathway in wheat roots: a role in aluminum toxicity. Plant Cell 7: 1913–1922

Katoh K, Kano Y, Masuda M, Onishi H, Fujiwara K (1998) Isolation and contraction of the stress fiber. Mol Biol Cell 9: 1919–1938

Ko KS, McCulloch CA (2000) Partners in protection: interdependence of cytoskeleton and plasma membrane in adaptations to applied forces. J Membr Biol 174: 85–95

Kochian LV (1995) Cellular mechanisms of aluminum toxicity and resistance in plants. Annu Rev Plant Physiol Plant Mol Biol 46: 237–260

Komis G, Apostolakos P, Galatis B (2002a) Hyperosmotic stress induced actin filament reorganization in leaf cells of *Chlorophytum comosum*. J Exp Bot 53: 1699–1710

– – – (2002b) Hyperosmotic stress induces formation of tubulin macrotubules in root-tip cells of *Triticum turgidum*: their probable involvement in protoplast volume control. Plant Cell Physiol 43: 911–922

– – – (2003) Actomyosin involved in the plasmolytic cycle: gliding movement of the deplasmolyzing protoplast. Protoplasma 221: 245–256

Krendel MF, Bonder EM (1999) Analysis of actin filament bundle dynamics during contact formation in live epithelial cells. Cell Motil Cytoskeleton 43: 296–309

Kudlicka K, Brown RM (1997) Cellulose and callose biosynthesis in higher plants. I. Solubilization and separation of (1 → 3)- and (1 → 4)-β-glucan synthase activities from mung bean. Plant Physiol 115: 643–656

Lindberg S, Strid H (1997) Aluminum induces rapid changes in cytosolic pH and free calcium and potassium concentrations in root protoplasts of wheat (*Triticum aestivum*). Physiol Plant 99: 405–414

Ma FJ, Ryan PR, Delhaize E (2001) Aluminium tolerance in plants and the complexing role of organic acids. Trends Plant Sci 6: 273–278

MacDdonald TL, Humphreys WG, Martin RB (1987) Promotion of tubulin assembly by aluminum ion in vitro. Science 236: 183–186

Matsumoto H (2000) Cell biology of aluminum toxicity and tolerance in higher plants. Int Rev Cytol 200: 1–46

McCormack BA, Gregory AC, Kerry ME, Smith C, Bolwell GP (1997) Purification of an elicitor induced glucan synthase (callose synthase) from suspension cultures of French bean (*Phaseolus vulgaris*): Purification and immunolocation of a probable M_r-65000 subunit of the enzyme. Planta 203: 196–203

Minocha R, McQuattie C, Fagerberg W, Long S, Noh EW (2001) Effects of aluminum in red spruce (*Picea rubens*) cell cultures: cell growth and viability, mitochondrial activity, ultrastructure and potential sites of intracellular aluminum accumulation. Physiol Plant 113: 486–498

Ostap ME (2002) 2,3-Butanedione monoxime (BDM) as a myosin inhibitor. J Muscle Res Cell Motil 23: 305–308

Panteris E, Apostolakos P, Quader H, Galatis B (2004) A cortical cytoplasmic ring predicts the division plane in vacuolated cells of *Coleus*: the role of actomyosin and microtubules in the establishment and function of the division site. New Phytol 163: 271–286

Papakonstanti EA, Vardaki EA, Stournaras C (2000) Actin cytoskeleton: a signaling sensor in cell volume regulation. Cell Physiol Biochem 10: 257–264

Rengel Z, Zhang W-H (2003) Role of dynamics of intracellular calcium in aluminium-toxicity syndrome. New Phytol 159: 295–314

Rout GR, Samantaray S, Das P (2001) Aluminium toxicity in plants: a review. Agronomie 21: 3–21

Ryan PR, Delhaize E, Jones DL (2001) Function and mechanism of organic anion exudation from plant roots. Annu Rev Plant Physiol Plant Mol Biol 52: 527–560

Sasaki M, Yamamoto Y, Matsumoto H (1997) Aluminum inhibits growth and stability of cortical microtubules in wheat (*Triticum aestivum*) roots. Soil Sci Plant Nutr 43: 469–472

Satoh M, Ishikawa T, Matsushima S, Naka M, Hidaka H (1987) Selective inhibition of catalytic activity of smooth muscle myosin light chain kinase. J Biol Chem 262: 7796–7801

Schwarzerová K, Zelenkova S, Nick P, Opatrny Z (2002) Aluminum-induced rapid changes in the microtubular cytoskeleton of tobacco cell lines. Plant Cell Physiol 43: 207–216

Shaw SL, Quatrano RS (1996) Polar localization of a dihydropyridine receptor on living *Fucus* zygotes. J Cell Sci 109: 335–342

Sivaguru M, Baluška F, Volkmann D, Felle HH, Horst WJ (1999a) Impacts of aluminum on the cytoskeleton of the maize root apex: short-term effects on the distal part of the transition zone. Plant Physiol 119: 1073–1082

– Yamamoto Y, Matsumoto H (1999b) Differential impacts of aluminium on microtubule organization depends on growth phase in suspension-cultured tobacco cells. Physiol Plant 107: 110–119

– Matsumoto H, Horst WJ (2000a) Control of the response to aluminium stress. In: Nick P (ed) Plant microtubules: potential for biotechnology. Springer, Berlin Heidelberg New York Tokyo, pp 103–120

– Fujiwara T, Šamaj J, Baluška F, Yang Z, Osawa H, Maeda T, Mori T, Volkmann D, Matsumoto H (2000b) Aluminum-induced 1 → 3-β-D-glucan inhibits cell-to-cell trafficking of molecules through plasmodesmata. A new mechanism of aluminum toxicity in plants. Plant Physiol 124: 991–1005

– Pike S, Gassmann W, Baskin TI (2003a) Aluminum rapidly depolymerizes cortical microtubules and depolarizes the plasma membrane: evidence that these responses are mediated by a glutamate receptor. Plant Cell Physiol 44: 667–675

– Ezaki B, He Z-H, Osawa H, Baluška F, Volkmann D, Matsumoto H (2003b) Aluminum-induced gene expression and protein localization of a cell wall-associated receptor kinase in *Arabidopsis*. Plant Physiol 132: 2256–2266

Strzelecka-Golaszewska H (2001) Divalent cations, nucleotides, and actin structure. Results Probl Cell Differ 32: 23–41

Szaszi K, Grinstein S, Orlowski J, Kapus A (2000) Regulation of the epithelial Na^+/H^+ exchanger isoform by the cytoskeleton. Cell Physiol Biochem 10: 265–272

Tominaga M, Yokota E, Sonobe S, Shimmen T (2000) Mechanism of inhibition of cytoplasmic streaming by a myosin inhibitor, 2,3-butanedione monoxime. Protoplasma 213: 46–54

Uemura S, Higuchi H, Olivares AO, De La Cruz EM, Ishiwata S (2004) Mechanochemical coupling of two substeps in a single myosin V motor. Nat Struct Mol Biol 11: 877–883

Vantard M, Blanchoin L (2002) Actin polymerization processes in plant cells. Curr Opin Plant Biol 5: 502–506

Verkhovsky AB, Svitkina TM, Borisy GG (1995) Myosin II filament assemblies in the active lamella of fibroblasts: their morphogenesis and role in the formation of actin filament bundles. J Cell Biol 131: 989–1002

Volkmann D, Baluška F (1999) Actin cytoskeleton in plants: from transport networks to signaling networks. Microsc Res Tech 47: 135–154

Zhang W-H, Ryan PR, Tyerman SD (2001) Malate-permeable channels and cation channels activated by aluminum in the apical cells of wheat roots. Plant Physiol 125: 1459–1472